THE TECHNICAL COOPERATION PROGRAM

SUBCOMMITTEE ON NON-ATOMIC MILITARY RESEARCH AND DEVELOPMENT

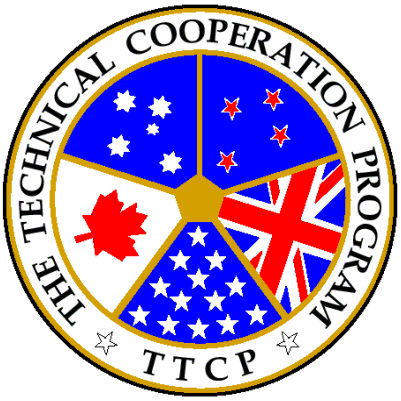

Verifying and validating the multistatic capability in ODIN using the advancing multistatic operational capabilities problem A 1.2.2

Prepared by
Talia Beech, Jackie Glister & Joshua Thistle (CAN)

CONTENTS

Verifying and validating the multistatic capability in ODIN using the advanced multistatic operational capabilities problem A 1.2.2

Talia Beech (DRDC CORA), Jackie Glister & Joshua Thistle (CFMWC MMSC),

1 AIM

The objective of this report is to document the effort of the Canadian Forces Maritime Warfare Centre (CFMWC) Defence Research Development Canada (DRDC) Centre for Operational Research and Analysis (CORA) and the CFMWC Maritime Modelling Simulation Cell (MMSC) to verify and validate (V&V) the recent upgrade to ODIN. The multistatic capability upgrade to ODIN was complete (including bug fixes) for the release of ODIN v.3.2.4 in November 2015. This study was conducted using results from the Advancing Multistatic Operational Capabilities (AMOC) Problem A 1.2.2 as defined in the Technical Cooperation Program (TTCP) Maritime Systems Group (MAR) Technical Panel 9 (TP9) report by Grimmett *et al* in 2012 [1]. The results of this study are presented in a series of transmission loss, reverberation and signal excess curves using notional data throughout this report.

2 BACKGROUND

Between 2008 and 2012 a subset of the TTCP MAR TP9 working group collaborated on the AMOC project, with the primary objective being cross-evaluation (or a V&V of international modelling and simulation toolsets) of multistatic tactical decision aids used within the TTCP communities. A secondary objective was to better understand the concepts of multistatics and also initiate a multistatic modelling capability within the nations involved. A scenario was developed by the working group of authors listed in [1] and was designated AMOC Problem A 1.2.2. Table 1 provides a list of the contributing AMOC participants, along with the acoustic propagation model used in their evaluation of AMOC Problem A.

Table 1 – AMOC organizations with their respective acoustic propagation models.

Organization	**Acoustic Propagation Model**
Defence Research and Development Canada Atlantic (DRDC A)	Comprehensive Acoustic System Simulation (CASS)
Defence Science and Technology Organisation (DSTO)	Comprehensive Acoustic System Simulation (CASS)
NATO Undersea Research Centre (NURC)	Energy-flux model developed at NURC
Naval Air Warfare Center (NAWC)	Acoustic System Performance Model (ASPM)
DRDC CORA & CFMWC	ODIN & DRDC Bellhop

Operational research analysts from DRDC CORA and CFMWC MMSC have been using the ODIN toolset since the early 2000s. ODIN is an underwater warfare simulation tool developed by Atlas Elektronik UK on behalf of the Ministry of Defence. ODIN has been identified by the Commander of the Royal Canadian Navy (RCN) as the approved model for force and tactical development [2] and is version controlled by the MMSC at the CFMWC. ODIN is a numerical modeling and simulation suite for simulating warfare scenarios in a dynamic UW domain. It is useful for modeling entities (platforms, threats, countermeasures, etc.) including components of those entities such as motion, shape, tactics, wake and acoustic signatures. ODIN can be used to enable entities to react to the actions of other entities and respond to the actions via a variety of tactical commands. It can also be used to model environments (such as specific geo-spatial locations), physical oceanographic conditions (such as shallow water or deep water environments) as well as temporally-specific periods. The results of this type of modeling can be used for a wide variety of naval requirements such as:

i. torpedo defence tactics development and effectiveness evaluation;
ii. anti-submarine warfare intelligence surveillance and reconnaissance tactics development and effectiveness evaluation;
iii. force development and acquisition;
iv. assessment of novel concepts; and
v. general threat assessment.

ODIN uses Bellhop [3] as its internal acoustic propagation model. Atlas Elektronik UK in concert with the Ministry of Defence have recently implemented a multistatic capability within ODIN, and the purpose of this study is to use the results presented by DRDC A [4] to V&V this multistatic capability. Further to verifying and validating this implementation in ODIN, the authors generated results using the DRDC A Bellhop, which was modified from the Internet version of Bellhop to make it compatible with DRDC A's Environmental Modelling Manager (EMM) [5]. This additional work serves to build more confidence in the performance of the multistatic implementation in ODIN as well as in the other models described in Table 1.

Following implementation of the multistatic capability in ODIN by Atlas Elektronik UK and the Ministry of Defence, several issues and areas for improvement were identified by the International ODIN User's Group (IOUG). The improvements to the ODIN multistatic capability are listed in the CFMWC statement of work to the proprietors of the ODIN software in [6]:

1. changing target strength data formats from UK specific formats to the international AMOC format;
2. changing reverberation profiles to become sensor specific rather than platform specific allowing fewer profiles to be created in many cases;
3. calculating and storing reverberation profiles for a 0 dB source level and adjusting for the true source level at the time of extraction reducing the workload on the caching system when source levels change;

4. correcting reverberation profile headers written to the output files to allow later re-use of calculated data;
5. allowing reverberation parameters to be sensor-specific rather than environment-specific;
6. allowing some environment input parameters to vary with frequency;
7. allowing user-control over conditions under which cached and requested reverberation profiles are considered to match;
8. updating default settings related to multistatics to ensure sensible results are achieved; and
9. addition of multistatic scattering models with dependence on incident vertical angle, scattered vertical angle and azimuthal angle.

The multistatic capability in ODIN allows for modelling target(s) detections using more than one transmitter and more than one receiver strategically placed, optimising detections. The advantages of multistatic sensing are well known to increase detection of targets using various sensing equipment in concert while minimising the false detections and reducing counter detection opportunities. These are not novel concepts and are well documented [7-10].

The scenario for AMOC Problem A 1.2.2 consists of a submarine transiting at a depth of 50 metres through a three by three grid of active multistatic sonobuoys. The scenario is separated into three categories (operations, systems, and environment) each specified with a level of complexity from one to three, for a total of 27 different variations. Variations of the scenario are designated Problem A *X.Y.Z.*, where *X*, *Y*, and *Z* are the complexity level of Operations, Systems, and Environment, respectively. Results are provided for Problem A 1.2.2 in the study conducted by DRDC A [4], which consist of complexity 1 operations, complexity 2 systems, and complexity 2 environment. A summary of AMOC Problem A *X.Y.Z* is given in Table 2, with the relevant sections outlined in bold.

Table 2 – Scenario summary for AMOC Problem A. Areas of interest for this study outlined in bold

Complexity	Operations	Systems	Environmental
Baseline (Complexity 1)	• 1 Tx, 3 Rx • 6 dB Omni TS • Buoy depth 30 m • Target speed 6 kts • Target depth 50 m	• Omni source • Omni receiver • FM pulse type • 300 s between pulses	• Isovelocity 1500 m/s • Fixed 95 m depth • No reverberation
Moderate (Complexity 2)	Same as baseline but: • 9 Tx, 9 Rx • Aspect dependent TS • Target speed 3 & 6 kts	Same as baseline but: • VLA source • DIFAR-like receiver • CW and FM pulse types	Same as baseline but: • Non-isovelocity SSP • Range independent bathymetry • Reverberation
Complex (Complexity 3)	Same as moderate but: • Buoy depth 30 & 60 m	Same as moderate but: • Planar receiver	Same as moderate but: • Range/azimuthal dependent bathymetry

3 SIMULATION SETUP

Table 2 provides a basic overview of the scenario. This section lays out some details of the scenario, with the remaining simulation parameters comprehensively described in Annex A.

3.1 Operations

The sonobuoys were positioned in a 20° rotated three by three square grid with a 10 km spacing centred on the operational area, as given in Table 3 (using ODIN's North-East-down coordinate system). For the baseline complexity scenario, only sonobuoy 8 was transmitting an active signal, while sonobuoys 7, 8, and 9 were receiving active signals. The target submarine operated at a constant depth of 50 m, heading of 318.4 °, and speed of 6 kts. Its path relative to the sonobuoy field can be seen in Figure 1, beginning in the bottom right of the diagram, passing through the sonobuoy field then through to the top left corner of the panel.

Table 3 – Sonobuoy placement for Problem A 1.2.2.

Sonobuoy	Y-Position (km)	X-Position (km)
1	37.18287	55.97672
2	46.57980	59.39693
3	55.97672	62.81713
4	40.60307	46.57980
5	50.00000	50.00000
6	59.39693	53.42020
7	44.02328	37.18287
8	53.42020	40.60307
9	62.81713	44.02328

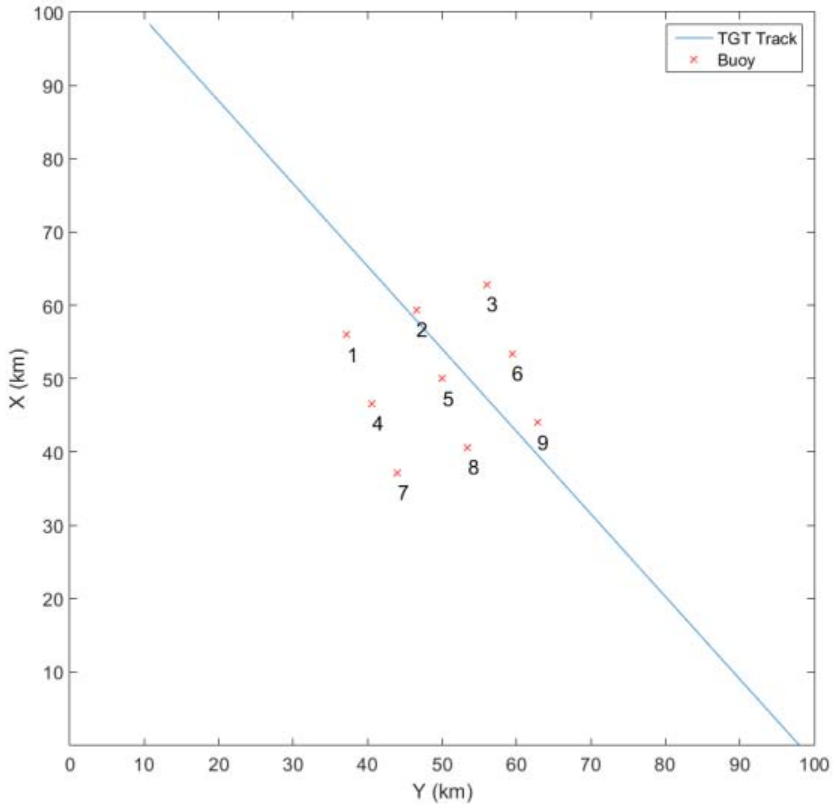

Figure 1 – Sonobuoy placement (shown as red xs) and target track (shown as the blue line) for AMOC Problem A 1.2.2.

3.2 Systems

The DRDC A study [4] only presented results using FM pulse types, while CW pulse types were left for future studies. The scenario specified the receive beams were to be horizontally steered to face the target for each ping. This would complicate the bistatic reverberation calculations as all steer angles would have a distinct reverberation profile. This specification was simplified in [4] through the use of only four cardioid beams oriented North, East, South and West.

3.3 Environment

The moderate complexity environment assumes range-independence with a depth dependent sound speed. The sound speed profile was pulled from Table 8 in the DRDC Atlantic paper [4] and is shown in Table 4 and graphically in Figure 2. Monostatic and bistatic reverberation were determined through the use of the acoustic propagation model as well as surface and bottom backwards scattering strength tables, which can be found in Annex A. A simplified bistatic scattering capability was implemented for a more direct comparison against AMOC organizations. Volume reverberation was ignored as it was assumed to be negligible compared to surface and bottom scattering. Reciprocity was assumed, so a single transmission loss profile was required for signals transmitted from the sonobuoys to the target as well as returned signals from reflection off of the target and received by the sonobuoys. Reciprocity could only be implemented using ODIN's *Tabular Bellhop* capability, which pre-computes a transmission loss profile to be used throughout the simulation. Acoustic propagation in both ODIN and DRDC A Bellhop was initialized using 5000 rays spread over a ±30 degree vertical angle with an incoherent summation of eigenrays. Transmission loss was computed at a range step interval of 200 m[1].

Table 4 – Sound speed profile for moderate complexity (2) environment.

Depth (m)	Sound Speed (m/s)
0.0	1527.0
10.0	1526.0
50.0	1485.0
95.0	1495.0

[1] The range step interval was chosen to be 200 m based on the computational memory limitations within ODIN itself. Smaller range step intervals were attempted, but caused a processing crash within ODIN. No significant effect on the study ensued.

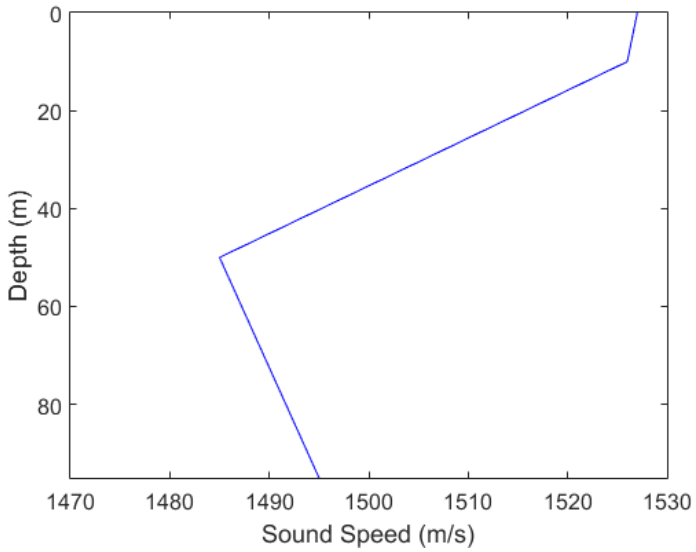

Figure 2 – Sound speed profile for moderate complexity (2) environment.

3.4 Sonar Equation

Preliminary comparisons of results from the AMOC study were conducted using signal excess [4]. The active sonar equation used for ODIN to calculate the signal excess is given below, where $\oplus$ indicates a power sum. Descriptions of the individual terms in the equation are provided in Table 5. The only terms in the sonar equation that vary during the simulation are both transmission loss terms and reverberation.

$$SE = SL - TL1 - TL2 + TS - \left((AN - DI) \oplus RL\right) + PG - RD - DF$$

Table 5 – Description of terms in sonar equation

Term	Description
SL	Source level of active sonar transmission (dB)
TL1	Transmission / propagation loss from the transmitter to the target (dB)
TL2	Transmission / propagation loss from the target to the receiver (dB)
TS	Target strength (dB)
AN	Ambient noise and bandwidth gain factor ($= AN_s + 10\log W$) (dB)
DI	Directivity index (dB)
RL	Reverberation level (dB)
PG	Processing gain for a correlated signal ($= 10\log(WT)$)
RD	Recognition differential (dB)
DF	Degradation factor accounting for other various losses (dB)
W	Active sonar bandwidth (Hz)
T	Processing time (s)

4 RESULTS

The results generated using ODIN were compared to the results presented by DRDC A [4], which were conducted using CASS, and the results generated using DRDC A Bellhop.

Figure 3 shows the transmission loss comparison as a function of range for a transmission at a depth of 30 m to a receiver at a depth of 50 m for the three models: CASS, DRDC Bellhop and ODIN. The sharp drop at approximately 57 km in the ODIN curve was determined to be non-physical. It is the result of the rays being suppressed beyond a specified maximum number of reflections in ODIN (set in the environmental input file and limited by internal memory restrictions). The results show a fair level of agreement between all three acoustic propagation models, but CASS generally predicts slightly decreased transmission loss levels (on the order of approximately 5 dB) with less variability,

with ODIN having slightly higher transmission loss and slightly more variability. The most variability in transmission loss is seen in the DRDC Bellhop model, with close to 20 dB variability in the 2-6 km ranges and the 47-51 km ranges. This increase in TL in the DRDC Bellhop model is likely due to non-physical limitations in the model, similar to ODIN. For more information on this curve, please refer to the DRDC report [4]. Variability within ODIN is fairly constant, along the order of 5 dB for the ranges studied. Reciprocity was assumed for the AMOC study, so an identical transmission loss profile was used for signals returning from the target depth of 50 m to the receivers at 30 m. The validity of this assumption was tested by generating the transmission loss for the return echo.

Figure 4 compares the transmission loss profile of the initial signal predicted by DRDC A to the profile of the return signal predicted by ODIN and DRDC A Bellhop (ignoring reciprocity), which shows a significant difference after 20 km. Intuitively, this flattening of the curves for both ODIN and DRDC Bellhop are likely due to the transmission loss transitioning from spherical spreading to cylindrical spreading. Figure 4 shows the CASS results from DRDC A, which used the same transmission loss from the source to the target and the target to the receiver. The initial transmission loss profile was used for both the transmitted and received signals in the simulations to determine signal excess, which is documented in Figures 8-11.

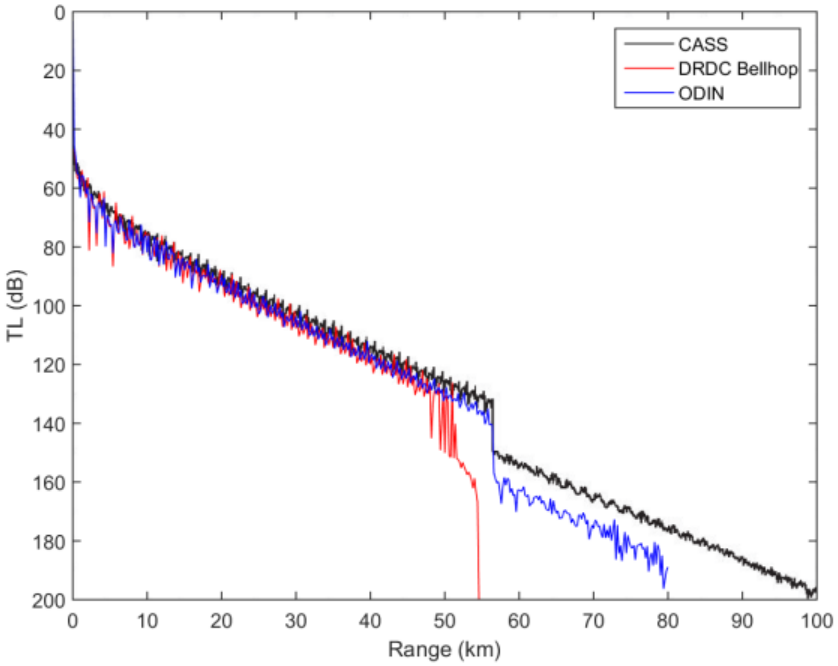

Figure 3 – Transmission loss comparison between CASS, DRDC A Bellhop, and ODIN from a transmitter at a depth of 30 m to a receiver at a depth of 50 m.

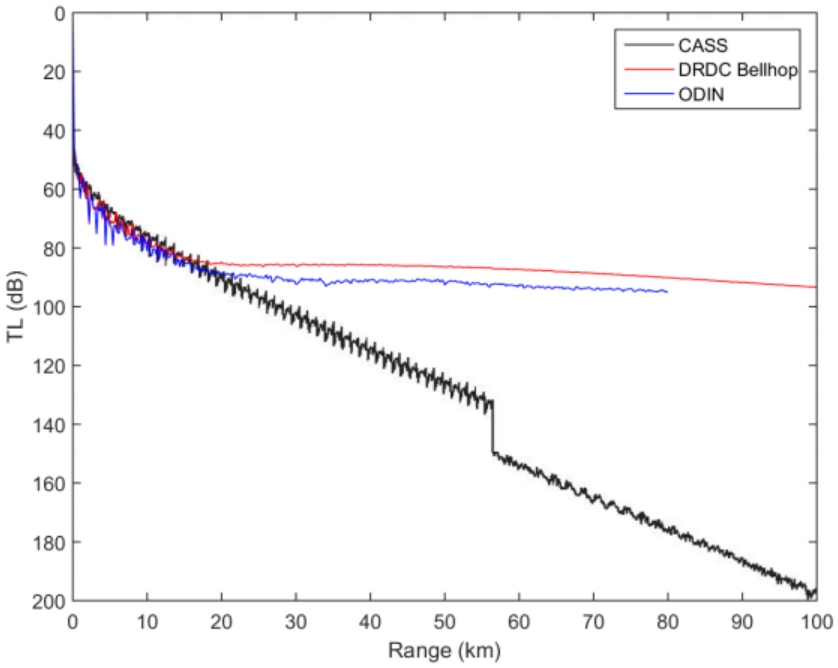

Figure 4 – Transmission loss comparison between CASS, DRDC A Bellhop, and ODIN from a transmitter at a depth of 50 m to a receiver at a depth of 30 m.

A comparison of the monostatic reverberation between ODIN, DRDC A Bellhop, and CASS is given in Figure 5. The three models predict a similar overall trend with short-term variations in the reverberation level having a time interval of approximately two seconds. The amplitude of these short-term variations, however, is significantly larger in the results predicted from ODIN, especially within the first 20 seconds. This was initially believed to be caused by having too few rays or eigenrays for the internal acoustic propagation model, but increasing these parameters did not produce a significant change. The DRDC Bellhop curve drops off at just after 70 seconds due to the model's hard-coded limitations. The characterization of the monostatic reverberation variation bands in terms of the time interval of the variations tends towards agreement across the three models, though the actual amplitude of the reverberation in ODIN is quite a bit larger than in the other two models, on the order of as much as five times in the first 20 seconds studied.

Predicted bistatic reverberation levels from ODIN (dashed lines) and CASS (solid lines) for all four beams (North (N), East (E), South (S) and West (W)) of sonobuoy 9 are given in Figure 6. The effects of the main blast can be seen by the initial plateau at the onset of reverberation at approximately 7.5 seconds. The comparison shows some inconsistency in the strength of the main blast, but the results from both models are well aligned after. The order of magnitude is at most

20 dB in the northerly direction and the smallest delta of approximately 10 dB occurs in the southerly direction during the main blast. Bistatic reverberation levels predicted by DRDC A Bellhop (solid lines) are also given in Figure 7 alongside those of ODIN (dashed lines). DRDC A Bellhop only accounts for surface and bottom scattering, and does not include the effects from the main blast. Beyond this initial difference the results are comparable. Bistatic reverberation is shown only for the four beams of sonobuoy 9 due to the symmetry of the sonobuoy placement. Equal reverberation levels are experienced by the beams from sonobuoy 7 (with a rearrangement of steer angles). The sharp drop in both bistatic and mono-static reverberation between 70 and 80 seconds is related to the non-physical spike in transmission loss (hard-coded for DRDC Bellhop and user-limited to avoid a memory crash in ODIN).

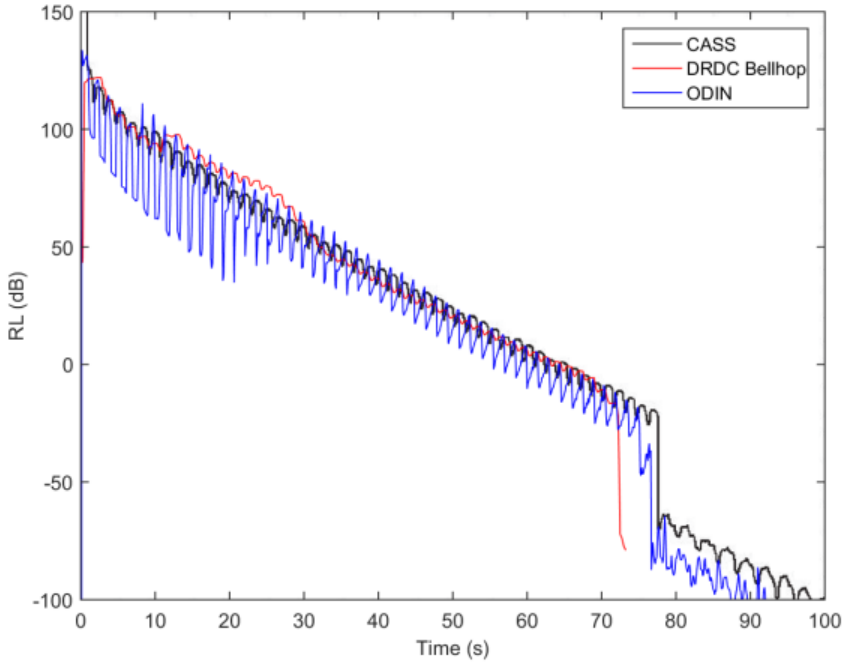

Figure 5 – Monostatic reverberation comparison for the three models: CASS, DRDC Bellhop and ODIN.

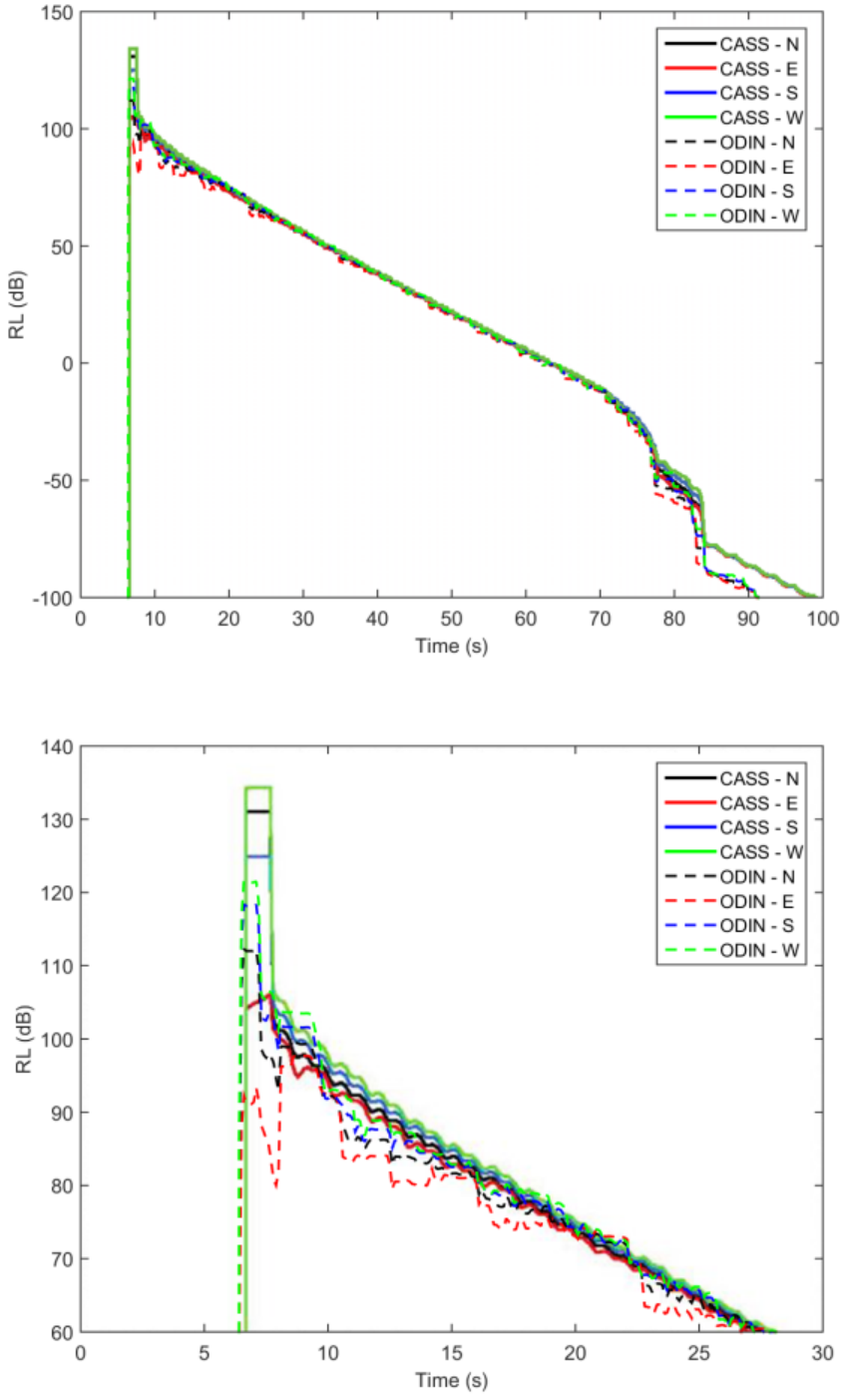

Figure 6 – Bistatic reverberation comparison between CASS and ODIN for all beams of sonobuoy 9. Enhanced view of top panel is presented on bottom panel.

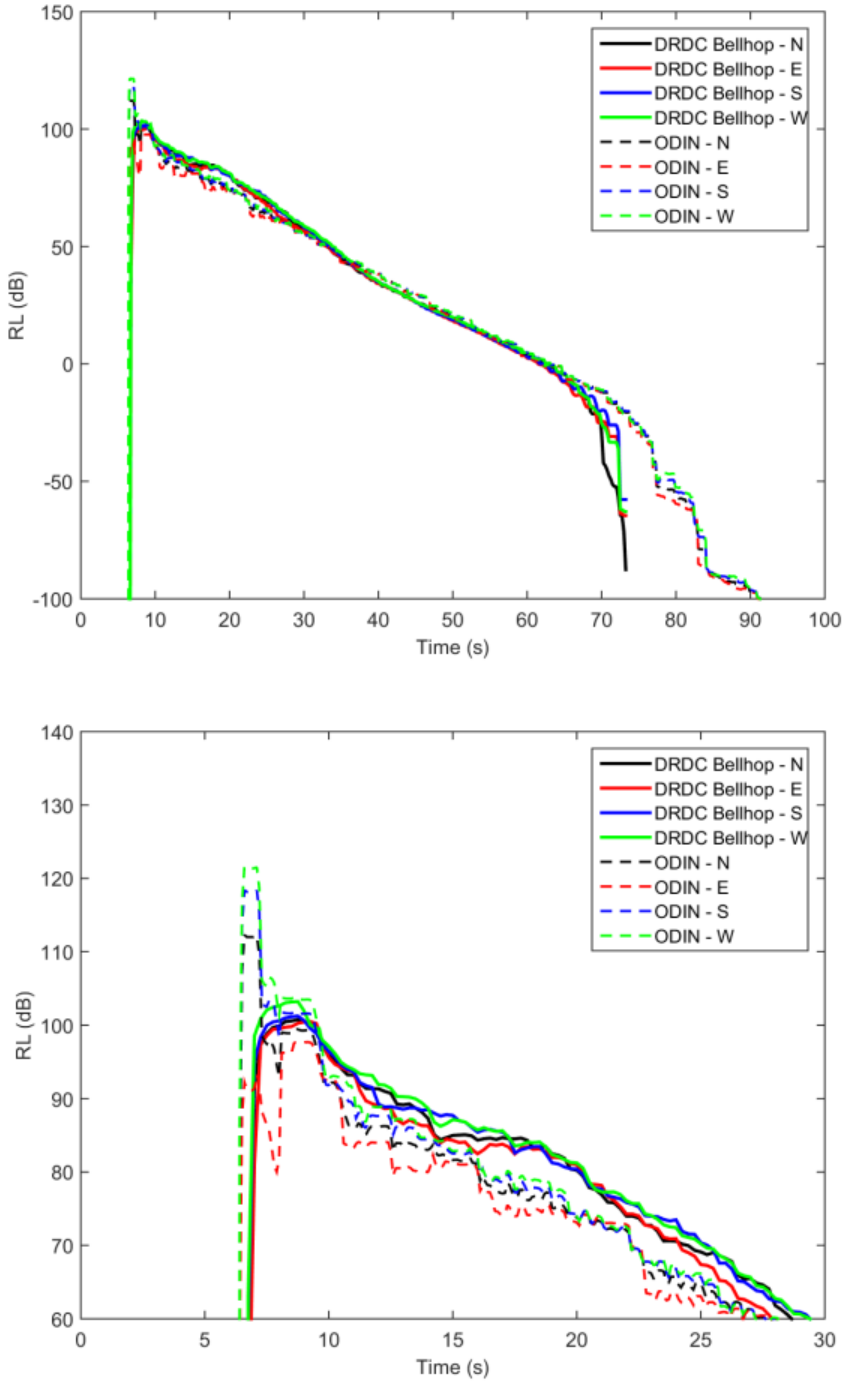

Figure 7 – Bistatic reverberation comparison between DRDC A Bellhop and ODIN for all beams of sonobuoy 9. Enhanced view of top panel is presented on bottom panel.

Predicted signal excess comparison between ODIN (CFMWC) and the AMOC organizations (DRDC A, DSTO, NURC and NAWC) for sonobuoys 7, 8, and 9

are given in Figure 8, Figure 9, and Figure 10, respectively. The overall profiles for the signal excess predicted from ODIN fit well within the range of results of the AMOC organizations, particularly with DRDC and DSTO. Results are slightly under-predicted in most areas which are likely a result of the slight over-prediction of transmission loss. The plot for signal excess for sonobuoy 7 (Figure 8) shows constant and expected results throughout the number of pings. Figure 9 shows that sonobuoy 8 experiences large fluctuations in the signal excess predictions as a result of the highly variable monostatic reverberation (please refer to Figure 5). Figure 10 gives the predictions for signal excess for sonobuoy 9 and shows a significant drop of signal excess during the closest point of approach of the target. This drop is caused by the main blast arriving at the same time as the target echo, as shown in Figure 6 & 7.ODIN has a capability to reject bistatic signals to prevent positive detection from a direct signal, but in this instance it could not be used as it likely would have rejected the target echo as well. Arrivals from the direct signal were filtered in post-processing to ensure signal excess levels were from the target echo only.

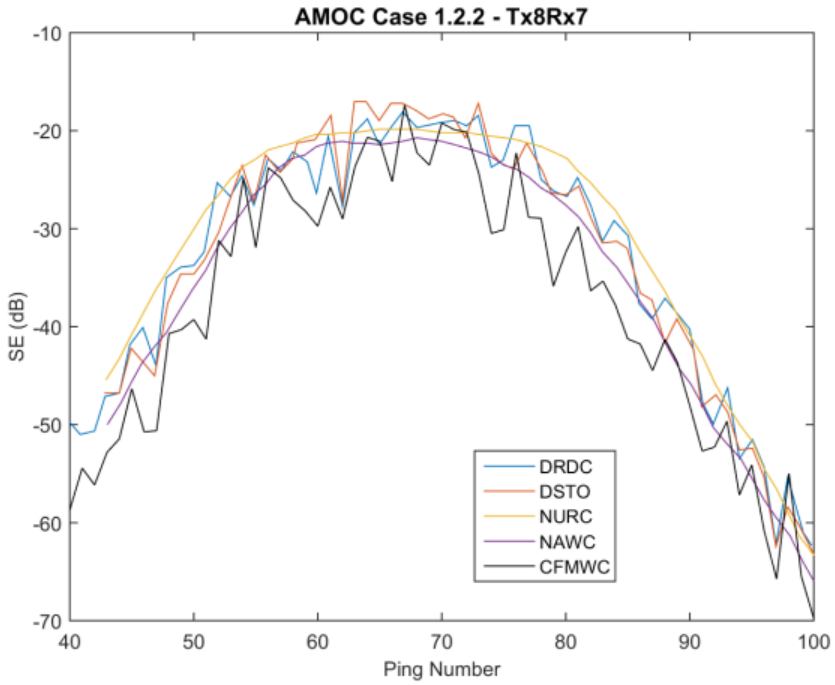

Figure 8 – Bistatic signal excess comparison of sonobuoy 7 from all organizations.

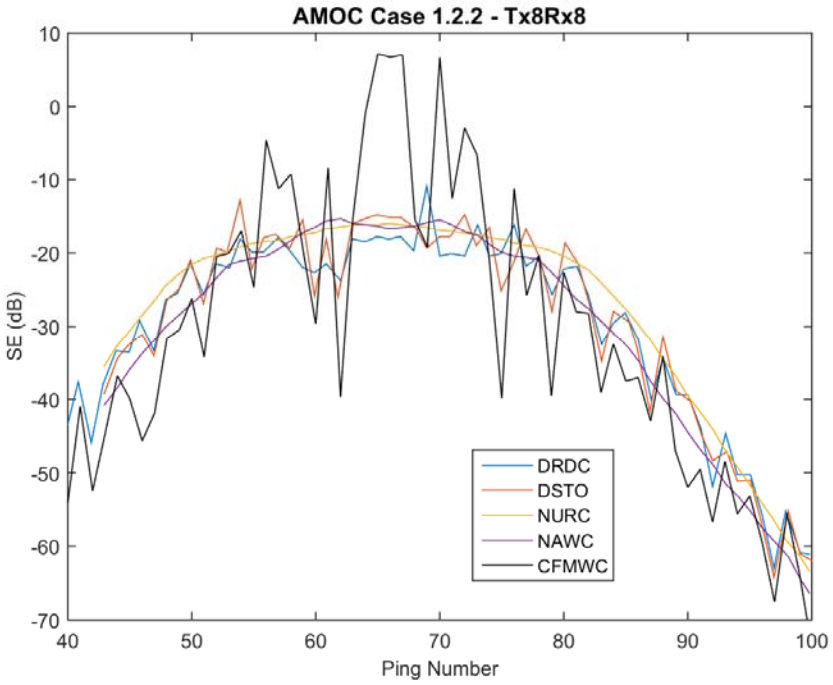

Figure 9 – Monostatic signal excess comparison of sonobuoy 8 from all organizations.

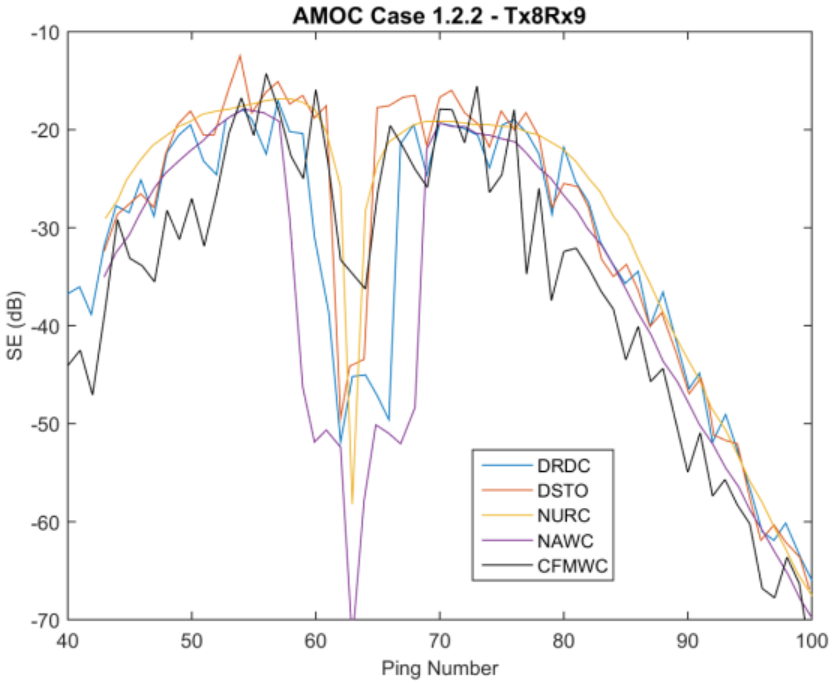

Figure 10 – Bistatic signal excess comparison of sonobuoy 9 from all organizations.

Signal excess encompasses several features, so it is more difficult to determine the cause for discrepancies when conducting comparisons and thus determine if

the multistatic capability was properly implemented. For a more direct comparison and to better understand the variation in signal excess between models, the transmission loss data predicted from [4] was then used as an input into the ODIN simulation, generating the results shown in Figure 11. The original transmission loss data was not available, so it was manually obtained from the figures with some degree of error. One can see from Figure 11 there is general agreement between the DRDC and CFMWC curves across the three sonobuoys, with the variations between outputs likely attributed to the inaccuracies of the method used to obtain the transmission loss data. This could only be done for the case ignoring reverberation as the reverberation profile presented in [4] was with respect to time, and could not be properly correlated with the transmission loss.

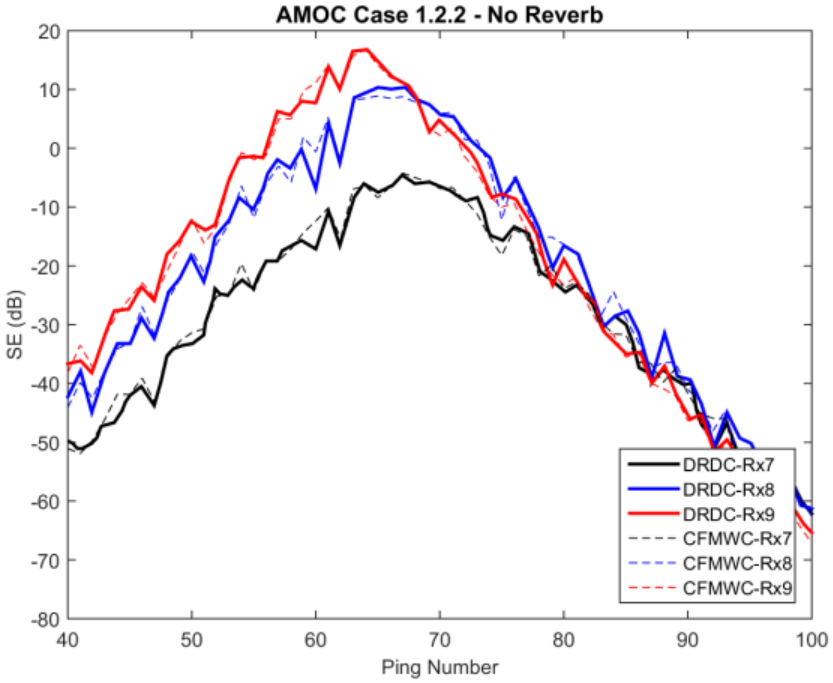

Figure 11 – Reverberation free signal excess comparison using equal transmission loss profiles.

5 SUMMATION

The transmission loss profile predicted by ODIN and DRDC A Bellhop were nearly identical as anticipated as the propagation models were both derived from Bellhop [4]. These transmission loss levels were comparable to those predicted by CASS, but were slightly increased on the order of 5 dB.

Monostatic reverberation predicted by ODIN followed the same overall trend as that predicted in [4], but had significantly increased amplitude of variation. The bistatic reverberation comparisons showed some variation in the reverberation level caused by the main blast, but were very consistent beyond that.

Bistatic signal excess levels predicted by ODIN throughout the simulation were similar to those of the AMOC organizations, but with a constant offset of approximately 5 dB below. Monostatic signal excess had a significant degree of variability caused by the reverberation levels. Results were very consistent between ODIN and DRDC A when using the transmission loss profile from [4] as input into ODIN, verifying the methodology used by ODIN to evaluate the sonar equation for multistatic scenarios. The previous discrepancies between the results generated from ODIN and the AMOC organizations were caused by the calculation of acoustic propagation, which is independent of multistatics.

ODIN and DRDC A Bellhop predicted a significantly different transmission loss levels for the return echo from the target to the receiver (as seen in Figure 4), suggesting that the assumption of reciprocity may not be valid. As the complexity level of this scenario is meant solely for validation of the multistatic capability of acoustic software, the validity in this assumption is irrelevant at this time.

6 RECOMMENDATION

Agreement in the performance of the ODIN toolset within a multistatic context has been reached and shown throughout this paper. More testing will be required once actual simulations are being run in ODIN to feed into any force development or tactical development initiatives at CFWMC. This testing should incorporate the testing of the acoustic propagation in ODIN and should be investigated further to determine the cause for the high variability in monostatic reverberation. If time becomes available, the use of ODIN's bi-static scattering model for reverberation could be explored to provide a basis for comparison with other bi-static scattering models, should they become available.

REFERENCES

1. Grimmet, D., Campbell, S., Frech, K., Fromm, D., Incze, B., Kelly, L., Krout, D., Maranda, B., Roger, B., Strode, C., Wood, G. and Zhang, Y. 2012. AMOC metric / products for level 1 cross-evaluation test scenario description v2.0 test problem A. TTCP MAR TP9. UNCLASSIFIED.

2. Maritime Modelling and Simulation (M&S) Policy, NAVORD 3771-14, April 2014. UNCLASSIFIED

3. Porter, M.B. and Liu, Y.C. 1994. Finite-Element Ray Tracing, Theoretical and Computational Acoustics – Vol 2, World Scientific Publishing Co. UNCLASSIFIED

4. Maranda, B. and Pecknold, S.P. 2012. Multistatic modeling. DRDC Atlantic TM 2012-260. UNCLASSIFIED

5. McCammon, D., 2010. Users Guide to BellhopDRDC_V4. DRDC Atlantic CR 2010-134. UNCLASSIFIED

6. Glister, J. and Atlas UK. 2013. Statement of work: ODIN Multistatic sonar, low frequency propagation and new boundary models. UNCLASSIFIED.

7. Naluai, N.K., Lauchle, G., Gabrielson and Joseph, J. 2007. Bi-static applications of intensity processing. Journal of Acoustic Society of America, 121 (4), pp. 1909–1915

8. Lucifredi, I. and Schmidt, H. 2006. Subcritical scattering from buried elastic shells. Journal of Acoustic Society of America, 120 (6), pp. 3566–3583, 2006

9. Bowen, J.I. and Mitnick, R.W. 1999. A Multistatic Performance Prediction Methodology. Johns Hopkins APL Technical Digest, v.2, No 3, pp. 424–431

10. Munafo, A. 2014. Addition of localization services to acoustic communication for enhanced navigation of AUVs in multi-static anti-submarine scenarios. Centre for Maritime Research and Experimentation. CMRE-FR-2014-012.

ABBREVIATIONS

AMOC	advancing multistatic operational capabilities
ASPM	acoustic system performance model
ASW	anti-submarine warfare
CASS	comprehensive acoustic system simulation
CFMWC	Canadian Forces Maritime Warfare Centre
CORA	Centre for Operational Research and Analysis
DRDC	Defence Research and Development Canada
DSTL	Defence Science & Technology Laboratory, UK
DSTO	Defence Science Technology Organisation, Australia
E	East
EMM	environmental modelling manager
IOUG	international ODIN user's group
MAR	maritime systems group
MMSC	maritime modelling and simulation cell
N	North
NAWC	Naval Air Warfare Center
NURC	NATO Undersea Research Centre
OA	operations analysis
OR	operations research
RCN	Royal Canadian Navy
RN	Royal Navy
S	South
TP9	technical panel 9
TTCP	The Technical Cooperation Program
V&V	verification and validation
W	West

DISTRIBUTION LIST
MAR TP-9

Dr Douglas Todoroff
MAR TP-9 Chairman
Acoustics Division, Code 7100
Naval Research Laboratory
4555 Overlook Ave., S.W.
Washington, D.C. 20375-5350
USA
douglas.todoroff@nrl.navy.mil

Dr David Liebing
MAR TP-9 Australian National Leader
Maritime Division, Defence Science & Technology Organisation
Building 79, PO Box 1500
Edinburgh SA 5111
Australia
david.liebing@dsto.defence.gov.au

Dr Dan Hutt
MAR TP-9 Canadian National Leader
Defence Research & Development Canada – Atlantic
PO Box 1012
Dartmouth, Nova Scotia B2Y 3Z7
Canada

Dr Nathaniel de Lautour
Defence Technology Agency
New Zealand Defence Force
Naval Base, Private Bag 32901
Devonport, Auckland
New Zealand

Mr Gary Wood
MAR TP-9 United Kingdom National Leader
Naval Systems Department
Defence Science & Technology Laboratory, Portsdown West
Portsdown Hill Road,
Fareham, Hampshire, PO17 6AD
United Kingdom

Mr Michael Vaccaro
MAR TP-9 United States National Leader
Office of Naval Research
875 North Randolph St., Suite 1425, Code 321US
Arlington VA 22203-1995
USA

ANNEX A

Details regarding AMOC Problem A 1.2.2 are provided below. Information related to higher complexity scenarios such as the aspect dependent target strength and range-dependent bathymetry were not included in this report as they were not implemented. Operational parameters dictate how the simulation is to be conducted, and include things such as placement of entities, speed and heading of the target, and simulation duration. Table A-1 provides the baseline (complexity 1) operational parameters used for this study (assuming a North-East-down coordinate system).

Table A-1 – Summary of operational parameters (complexity 1).

Description	Value
Operational area	100 km x 100 km
Ping interval	300 s
Simulation duration	710 mins
Transmit buoy	8
Receive buoys	7,8,9
Sonobuoy depth	30 m
Sonobuoy positions	See **Table 3**
Target initial position	X = 0 km, Y = 98 km
Target speed	6 kts
Target heading	318.4° (clockwise from North)
Target depth	50 m
Target strength	6 dB Omni

All specifications for how the sonobuoys operate, such as source level, pulse length, and directivity index, are provided in the system parameters, shown in Table A-2.

Table A-2 – Summary of system parameters (complexity 2).

Description	Value
Transmission source level	210 dB
Pulse type	FM only
Sonar channel centre frequency	1800 Hz
Sonar channel bandwidth	100 Hz
Pulse length	2.0 s
Recognition differential	12 dB
Directivity index	5 dB
Degradation factor	3 dB
Horizontal receiver beam pattern	Cardioid (see **Figure A-1**)
Vertical receiver beam pattern	Cardioid (see **Figure A-1**)
Horizontal receiver steer direction	N,E,S,W (four beams)
Vertical receiver steer direction	0°
Horizontal transmit beam pattern	Omni
Vertical transmit beam pattern	8 transducers at λ/2 linear spacing (see **Figure A-2**)
Horizontal transmit steer direction	Omni
Vertical transmit steer direction	0°

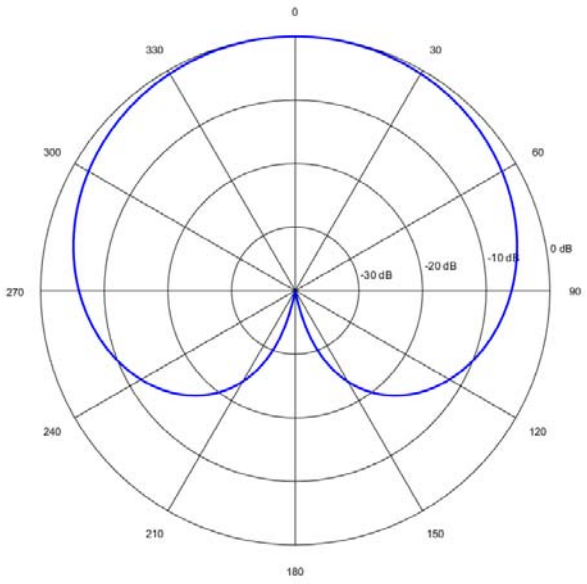

Figure A-1 – Cardioid beam pattern

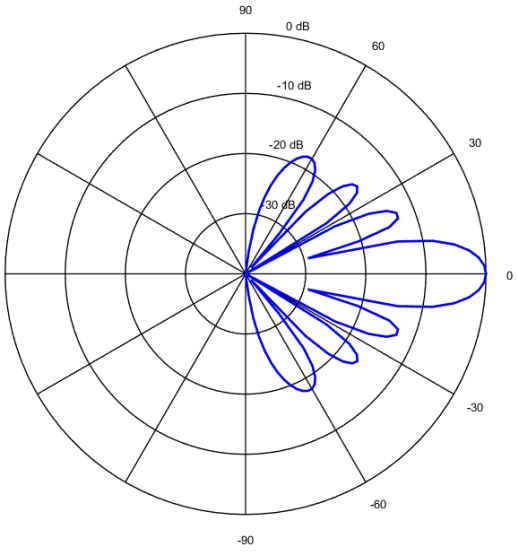

Figure A-2 – Vertical beam pattern of the transmit array

Environmental parameters include things such as bathymetry, sound speed profile, and surface and bottom boundary conditions. Table A-3 provides the

moderate (complexity 2) environmental parameters used for this study. Note that the given ambient noise level is spectral (AN_s), and not equal to the ambient noise parameter used in the equation for signal excess ($AN = AN_s + 10\log W$).

Table A-3 – Summary of Environmental parameters (complexity 2) [D]

Description	Value
Spectral ambient noise (AN_s)	60 dB rel. 1 μPa^2/Hz
Absorption coefficient	0.12 dB/km
Wind Speed	15 knots
Bathymetry	Fixed depth of 95 m
South speed profile	See Table 4
Forward surface scattering model	Kirchoff approximation (see Table A-4)
Forward bottom scattering model	Rayleigh reflection (see Table A-5)
Backward surface scattering model	Chapman-Harris (see Table A-6)
Backward bottom scattering model	Lambert's Law (see Table A-7)
Backward bottom scattering strength ($10\log\mu$)	-22.8 dB/m^2

Forward surface scattering strength accounts for the degradation of the signal when it reflects off of the surface of the water, and is used in the calculation of transmission loss. The forward surface scattering strength used for this scenario is given by the Kirchhoff approximation with a cap of -9.0 dB [4].

$20\log\left(e^{-2k^2h^2\sin^2\theta}\right)$, where

$k = \frac{2\pi f}{c}$ and

$h = (0.0247/4)U^2$

where θ is the grazing angle, and U is the wind speed in m/s. The forward surface scattering strength calculated at a wind speed of 15 knots is given in Table A-4.

Table A-4 – Forward surface scattering strength. Wind speed is 15 kts.

Grazing	Strength	Grazing	Strength

Angle (°)	(dB)	Angle (°)	(dB)
0.0	-0.0000	8.0	-2.7999
0.5	-0.011008	8.5	-3.1582
1.0	-0.044029	9.0	-3.5375
1.5	-0.099054	9.5	-3.9378
2.0	-0.17606	10.0	-4.3589
2.5	-0.27504	10.5	-4.8006
3.0	-0.39594	11.0	-5.2630
3.5	-0.53874	11.5	-5.7457
4.0	-0.7034	12.0	-6.2487
4.5	-0.88985	12.5	-6.7718
5.0	-1.0981	13.0	-7.3149
5.5	-1.3279	13.5	-7.8778
6.0	-1.5794	14.0	-8.4602
6.5	-1.8525	14.5	-9.0000
7.0	-2.1469	15.0	-9.0000
7.5	-2.4628	>15.0	-9.0000

Forward surface scattering strength accounts for the degradation of the signal when it reflects off of the seabed. The strength is given by Rayleigh reflection with additional scattering due to surface roughness [4], and is shown in Table A-5.

Table A-5 – Forward bottom scattering strength.

Grazing Angle (°)	Strength (dB)	Grazing Angle (°)	Strength (dB)	Grazing Angle (°)	Strength (dB)	Grazing Angle (°)	Strength (dB)
0	-0.0000	23	-4.5607	46	-16.2730	69	-22.8180
1	-0.1350	24	-5.0749	47	-16.6270	70	-23.0160

2	-0.2772	25	-5.7022	48	-16.9750	71	-23.2050
3	-0.4242	26	-6.4206	49	-17.3160	72	-23.3860
4	-0.5741	27	-7.1670	50	-17.6520	73	-23.5580
5	-0.7255	28	-7.8886	51	-17.9820	74	-23.7220
6	-0.8775	29	-8.5654	52	-18.3060	75	-23.8760
7	-1.0299	30	-9.1959	53	-18.6240	76	-24.0200
8	-1.1827	31	-9.7852	54	-18.9370	77	-24.1560
9	-1.3365	32	-10.3390	55	-19.2430	78	-24.2810
10	-1.4922	33	-10.8630	56	-19.5430	79	-24.3980
11	-1.6508	34	-11.3630	57	-19.8360	80	-24.5040
12	-1.8136	35	-11.8410	58	-20.1240	81	-24.6010
13	-1.9820	36	-12.3010	59	-20.4040	82	-24.6870
14	-2.1576	37	-12.7450	60	-20.6790	83	-24.7640
15	-2.3420	38	-13.1750	61	-20.9460	84	-24.8310
16	-2.5372	39	-13.5940	62	-21.2060	85	-24.8870
17	-2.7455	40	-14.0020	63	-21.4590	86	-24.9330
18	-2.9698	41	-14.4000	64	-21.7050	87	-24.9690
19	-3.2142	42	-14.7900	65	-21.9430	88	-24.9950
20	-3.4844	43	-15.1710	66	-22.1740	89	-25.0110
21	-3.7889	44	-15.5450	67	-22.3960	90	-25.0160
22	-4.1410	45	-15.9120	68	-22.6110		

Backward surface scattering strength accounts for the degradation of a scattered signal that has reflected off of the surface boundary, and is used in the calculation of reverberation. The surface scattering strength is given by the Chapman-Harris model [3]:

$3.3\beta \log\left(\frac{6\theta}{\pi}\right) - 42.4 \log \beta + 2.6$, where

$\beta = 158\left(Uf^{1/3}\right)^{-0.88}$,

where θ is the incident grazing angle in radians, U is the wind speed in knots, and f is the frequency in Hertz. Table A-6 provides the backward bottom

scattering strength calculated using a frequency of 1800 Hz and a wind speed of 15 knots.

Table A-6 – Backward surface scattering strength at 1800 Hz and a wind speed of 15 kts.

Grazing Angle (°)	Strength (dB)	Grazing Angle (°)	Strength (dB)	Grazing Angle (°)	Strength (dB)	Grazing Angle (°)	Strength (dB)
0	-1000	21	-38.9583	45	-30.5346	69	-25.8101
0.01	-123.5080	22	-38.4441	46	-30.2916	70	-25.6511
0.1	-98.0585	23	-37.9528	47	-30.0539	71	-25.4943
0.5	-80.2698	24	-37.4824	48	-29.8212	72	-25.3397
1	-72.6086	25	-37.0312	49	-29.5933	73	-25.1873
2	-64.9474	26	-36.5977	50	-29.3701	74	-25.0369
3	-60.4659	27	-36.1806	51	-29.1512	75	-24.8886
4	-57.2863	28	-35.7786	52	-28.9366	76	-24.7422
5	-54.8199	29	-35.3908	53	-28.7260	77	-24.5977
6	-52.8048	30	-35.0161	54	-28.5194	78	-24.4551
7	-51.1010	31	-34.6537	55	-28.3166	79	-24.3143
8	-49.6251	32	-34.3027	56	-28.1175	80	-24.1752
9	-48.3233	33	-33.9626	57	-27.9218	81	-24.0379
10	-47.1587	34	-33.6327	58	-27.7296	82	-23.9023
11	-46.1053	35	-33.3123	59	-27.5407	83	-23.7683
12	-45.1436	36	-33.0009	60	-27.3549	84	-23.6360
13	-44.2589	37	-32.6981	61	-27.1722	85	-23.5052
14	-43.4398	38	-32.4033	62	-26.9925	86	-23.3759
15	-42.6772	39	-32.1162	63	-26.8156	87	-23.2481
16	-41.9639	40	-31.8364	64	-26.6416	88	-23.1218
17	-41.2938	41	-31.5635	65	-26.4702	89	-22.9969
18	-40.6621	42	-31.2971	66	-26.3015	90	-22.8734
19	-40.0645	43	-31.0371	67	-26.1353		
20	-39.4976	44	-30.7830	68	-25.9715		

The backward bottom scattering strength is given by the angle-separable form of Lambert's law [4]:

$$10\log(\mu \sin\theta_i \sin\theta_r) = 10\log\mu + 10\log(\sin\theta_i \sin\theta_r),$$

where μ is the bottom scattering strength in m^{-2}, θ_i is the incident grazing angle, and θ_r is the reflected grazing angle. As a simplification for the AMOC organizations, the incident and grazing angles were assumed to be equal (monostatic reverberation) [4]. Although ODIN has a bistatic scattering capability, this simplification was implemented for a more direct comparison against the AMOC organizations. For moderate complexity environment parameters, the bottom scattering strength in decibels ($10\log\mu$) was assumed to be -22.8 dB/m^2, generating the scattering strength values given in Table A-7.

Table A-7 – Backward bottom scattering strength

Grazing Angle (°)	Strength (dB)	Grazing Angle (°)	Strength (dB)	Grazing Angle (°)	Strength (dB)	Grazing Angle (°)	Strength (dB)
0	-1000	21	-31.7134	45	-25.8103	69	-23.3970
0.01	-97.9625	22	-31.3285	46	-25.6613	70	-23.3403
0.1	-77.9625	23	-30.9624	47	-25.5175	71	-23.2866
0.5	-63.9832	24	-30.6137	48	-25.3785	72	-23.2359
1	-57.9629	25	-30.2810	49	-25.2444	73	-23.1881
2	-51.9436	26	-29.9632	50	-25.1149	74	-23.1432
3	-48.4240	27	-29.6591	51	-24.9899	75	-23.1011
4	-45.9283	28	-29.3678	52	-24.8694	76	-23.0619
5	-43.9941	29	-29.0886	53	-24.7530	77	-23.0255
6	-42.4153	30	-28.8206	54	-24.6408	78	-22.9919
7	-41.0821	31	-28.5632	55	-24.5327	79	-22.9611
8	-39.9289	32	-28.3158	56	-24.4285	80	-22.9330
9	-38.9134	33	-28.0778	57	-24.3282	81	-22.9076
10	-38.0066	34	-27.8488	58	-24.2316	82	-22.8849
11	-37.1880	35	-27.6282	59	-24.1387	83	-22.8650
12	-36.4424	36	-27.4156	60	-24.0494	84	-22.8477
13	-35.7582	37	-27.2107	61	-23.9636	85	-22.8331
14	-35.1265	38	-27.0132	62	-23.8813	86	-22.8212
15	-34.5401	39	-26.8226	63	-23.8024	87	-22.8119
16	-33.9932	40	-26.6387	64	-23.7268	88	-22.8053
17	-33.4813	41	-26.4611	65	-23.6545	89	-22.8013
18	-33.0004	42	-26.2898	66	-23.5854	90	-22.8000
19	-32.5472	43	-26.1243	67	-23.5195		
20	-32.1190	44	-25.9646	68	-23.4567		